

A comparative study of 4D-VAR and a 4D Ensemble Kalman Filter: perfect model simulations with Lorenz-96

By ELANA J. FERTIG*, JOHN HARLIM and BRIAN R. HUNT, *Institute for Physical Science and Technology and Department of Mathematics, University of Maryland, College Park, MD 20742, USA*

(Manuscript received 7 April 2006; in final form 22 August 2006)

ABSTRACT

We formulate a four-dimensional Ensemble Kalman Filter (4D-LETKF) that minimizes a cost function similar to that in a 4D-VAR method. Using perfect model experiments with the Lorenz-96 model, we compare assimilation of simulated asynchronous observations with 4D-VAR and 4D-LETKF. We find that both schemes have comparable error when 4D-LETKF is performed sufficiently frequently and when 4D-VAR is performed over a sufficiently long analysis time window. We explore how the error depends on the time between analyses for 4D-LETKF and the analysis time window for 4D-VAR.

1. Introduction

Operational data assimilation schemes traditionally have assimilated available observations as though they, or their innovations from the background forecast, occurred at the analysis time. With a growing number of observations from instruments such as satellites, many observations are available between analysis times. However, employing three-dimensional data assimilation schemes to match the frequency of these asynchronous observations would be prohibitively expensive and could introduce imbalances in the resulting analysis states. New generations of data assimilation schemes, most notably the 4D-VAR and Ensemble Kalman Filter (EnKF) techniques, are able to more accurately take into account the timing of asynchronous observations.

One approach to assimilating observations at various time is 4D-VAR (see Le Dimet and Talagrand, 1986; Courtier et al., 1994; Rabier et al., 1998, 2000). This assimilation system is currently the operational data assimilation scheme at the European Centre for Medium-Range Weather Forecasts and Meteo-France, and being developed for operation at centres including the Canadian Meteorological Centre and the Japan Meteorological Agency. ‘Strong constraint’ 4D-VAR seeks a model trajectory that best fits the available observations during a specified time window before the analysis time.

Another developing approach to data assimilation is the EnKF technique (Evensen, 1994; Burgers et al., 1998; Houtekamer and

Mitchell, 1998; Anderson, 2001; Bishop et al., 2001; Whitaker and Hamill, 2002; Ott et al., 2004; Zupanski, 2005). These schemes evolve an ensemble of model trajectories to estimate background uncertainty. Though not yet operational, experiments such as those of Houtekamer et al. (2005), Szunoygh et al. (2005), and Whitaker et al. (2004) have shown the potential of EnKF for operational data assimilation. In these implementations of EnKF on operational models, observations are still assimilated as though they were taken at the analysis time. As Lorenc (2003) points out, when assimilating asynchronous observations with EnKF, one should use the time sequence of ensemble states between analysis times to account for model state correlations in time as well as space. In this way, Evensen and van Leeuwen (2000), Anderson (2001) and Hunt et al. (2004) extend EnKF to accurately assimilate asynchronous observations at the correct time. Their methods have been successfully applied to operational models by Houtekamer and Mitchell (2006), Szunoygh and Kostelich (2006, personal communication) and Whitaker et al. (2006).

In this paper, we present 4D-LETKF, a simplified version of the four-dimensional Ensemble Kalman Filter in Hunt et al. (2004), and compare it to 4D-VAR in a perfect model scenario using the Lorenz-96 system (Lorenz, 1996). In Section 2, we describe our implementation of 4D-VAR, and then derive 4D-LETKF using a modification of the 4D-VAR cost function. In Section 3, we describe our experimental design and present our numerical results. We find that the two methods yield similar results when the time between analysis is short enough for 4D-LETKF and when the analysis time window is long enough for 4D-VAR and we discuss our results further in Section 4.

*Corresponding author.

e-mail: ejfertig@math.umd.edu

DOI: 10.1111/j.1600-0870.2006.00205.x

2. Formulation

2.1. 4D-VAR

Since we consider a perfect model scenario in this paper, we formulate here a strong constraint 4D-VAR scheme. It seeks an initial condition close to the background state (determined by the prior analysis) from which the resulting exact model trajectory remains closest to the observations over the analysis time window, $[t_0, t_n]$. More precisely, it minimizes a cost function:

$$J(\mathbf{x}(t_0)) = \frac{1}{2} [\mathbf{x}(t_0) - \mathbf{x}^b]^\top \mathbf{B}^{-1} [\mathbf{x}(t_0) - \mathbf{x}^b] + \frac{1}{2} \sum_{l=0}^n \{y_l^o - H_l[\mathbf{x}(t_l)]\}^\top \mathbf{R}_l^{-1} \{y_l^o - H_l[\mathbf{x}(t_l)]\} \quad (1)$$

where \top denotes the transpose, $\mathbf{x}(t_0)$ is an m -dimensional the model state at the start of the analysis window. The model state at each observation time is obtained by integrating the non-linear model from $\mathbf{x}(t_0)$. \mathbf{x}^b is the the m -dimensional background forecast at the same time and \mathbf{B} is an $m \times m$ background error covariance matrix, which is typically constant, homogeneous and isotropic. The observation state at time t_l is given by the s_l -dimensional vector y_l^o . \mathbf{R}_l is the associated $s_l \times s_l$ observation error covariance matrix, for $l = 0, \dots, n$. The observation operator, H_l , maps the model state $\mathbf{x}(t_l)$ to the observation space at time t_l . For this formulation, observations taken at different times are assumed to have uncorrelated errors.

The cost J is only a function of the initial model state, $\mathbf{x}(t_0)$. Therefore, once we determine $\mathbf{x}(t_0)$ that minimizes the total cost J , the integrated state $\mathbf{x}(t_n)$ is the 4D-VAR analysis at time t_n . For this study, we obtain the minimum using a BFGS algorithm adapted from Numerical Recipes in Fortran (Press et al., 1992, p. 418). This algorithm requires the gradient of the cost function, which we compute using the adjoint technique presented in Lawson et al. (1995). For large systems, Hessian pre-conditioning is often employed to ensure that the minimization algorithm converges quickly on an accurate state. In this study, we judged pre-conditioning to be unnecessary because here the BFGS algorithm converges to the minimum state quickly (generally after about 20 iterations).

2.2. 4D-LETKF

EnKF replaces the time-independent background error covariance matrix \mathbf{B} with a time-dependent sample covariance matrix $\mathbf{P}^b = (k-1)^{-1} \mathbf{X}^b (\mathbf{X}^b)^\top$, where \mathbf{X}^b is an $m \times k$ matrix of background ensemble perturbations. That is,

$$\mathbf{X}^b = [\mathbf{x}^{b(1)} - \bar{\mathbf{x}}^b | \mathbf{x}^{b(2)} - \bar{\mathbf{x}}^b | \dots | \mathbf{x}^{b(k)} - \bar{\mathbf{x}}^b], \quad (2)$$

where $\mathbf{x}^{b(i)}$ denotes the i th ensemble member and $\bar{\mathbf{x}}^b$ denotes the ensemble mean. In 4D-LETKF, the deviation of a model solution $\mathbf{x}(t)$ from the background mean state $\bar{\mathbf{x}}^b(t)$ is approximated between analysis times by a linear combination of the background

ensemble perturbations by

$$\mathbf{x}(t) \approx \bar{\mathbf{x}}^b(t) + \mathbf{X}^b(t) \mathbf{w}, \quad (3)$$

where $\mathbf{w} \in \mathbf{IR}^k$ is a time-independent weight vector. As in Hunt et al. (2004), the analysis determines which weight vector makes this linear combination ‘best fit’ the observations over the analysis time window, in the sense of minimizing a cost function like (1).

The projection of $\mathbf{x}(t)$ to the observation space at time t_l is approximated by:

$$H_l(\mathbf{x}(t_l)) \approx H_l(\bar{\mathbf{x}}^b(t_l) + \mathbf{X}^b(t_l) \mathbf{w}) \approx H_l(\bar{\mathbf{x}}^b(t_l)) + \mathbf{Y}_l^b \mathbf{w}. \quad (4)$$

The i th column vector of the $s_l \times k$ matrix \mathbf{Y}_l^b is defined to be $H_l(\mathbf{x}^{b(i)}(t_l)) - H_l(\bar{\mathbf{x}}^b(t_l))$, where $H_l(\bar{\mathbf{x}}^b(t_l))$ represents the ensemble mean of the projection of the background state on observation space.

Replacing \mathbf{B} by $\mathbf{P}^b(t_0)$ and \mathbf{x}^b by $\bar{\mathbf{x}}^b(t_0)$ and substituting approximations (3) and (4) into the cost function (1) yields the modified cost function:

$$\tilde{J}(\mathbf{w}) = \frac{1}{2} (k-1) \mathbf{w}^\top \mathbf{w} + \frac{1}{2} \sum_{l=1}^n [y_l^o - H_l(\bar{\mathbf{x}}^b(t_l)) - \mathbf{Y}_l^b \mathbf{w}]^\top \times \mathbf{R}_l^{-1} [y_l^o - H_l(\bar{\mathbf{x}}^b(t_l)) - \mathbf{Y}_l^b \mathbf{w}]. \quad (5)$$

Here, the m -dimensional minimization problem is reduced to a k -dimensional problem, reducing the cost of implementation if the ensemble size k is less than the number of model variables m .

The minimum of (5) occurs at

$$\mathbf{w}^a = \tilde{\mathbf{P}}^a \left[\sum_{l=1}^n \mathbf{Y}_l^{b\top} \mathbf{R}_l^{-1} (y_l^o - H_l(\bar{\mathbf{x}}^b(t_l))) \right], \quad (6)$$

where $\tilde{\mathbf{P}}^a$ is the $k \times k$ matrix given by:

$$\tilde{\mathbf{P}}^a = \left[(k-1) \mathbf{I} + \sum_{l=1}^n \mathbf{Y}_l^{b\top} \mathbf{R}_l^{-1} \mathbf{Y}_l^b \right]^{-1}. \quad (7)$$

These equations correspond to the Kalman filter analysis mean and covariance equations; here the background mean and covariance for \mathbf{w} are $\mathbf{0}$ and $(k-1)^{-1} \mathbf{I}$, respectively. Now, the model state corresponding to (6) is the mean analysis state:

$$\bar{\mathbf{x}}^a = \bar{\mathbf{x}}^b + \mathbf{X}^b \mathbf{w}^a, \quad (8)$$

The analysis ensemble is generated as follows:

$$\mathbf{x}^{a(i)} = \bar{\mathbf{x}}^a + \mathbf{X}^b \mathbf{W}^{(i)}. \quad (9)$$

where $\mathbf{W}^{(i)}$ is the i th column of the matrix $\mathbf{W} = [(k-1)\tilde{\mathbf{P}}^a]^{1/2}$. The forecasts from these analysis ensemble states are then used for the next analysis as the background ensemble states.

We remark that a cost function similar to (5), but without the linear approximation (4) to the observation operator, is used in the Maximum Likelihood Ensemble Filter (Zupanski, 2005). The analysis (6)–(9) is equivalent to the Ensemble Transform

Kalman Filter (Bishop et al., 2001) with the Centred Spherical Simplex Ensemble (Wang et al., 2004). It is also equivalent, though formally less similar, to the analysis described in Hunt et al. (2004) and Ott et al. (2004). In this paper, the analysis is performed locally like in Ott et al. (2004), as described in the next section.

3. Results

We test both 4D-VAR and 4D-LETKF on Lorenz-96, a toy model with variable \mathbf{x} in m -equally spaced points around a circle of constant latitude. The j th component is propagated in time following differential equation:

$$\frac{d\mathbf{x}_j}{dt} = \frac{1}{120}[(\mathbf{x}_{j+1} - \mathbf{x}_{j-2})\mathbf{x}_{j-1} - \mathbf{x}_j + F] \quad (10)$$

where $j = 1, \dots, m$ represents the spatial coordinate ('longitude').

Following Lorenz (1996), like the study of Ott et al. (2004), we choose the external forcing to be $F = 8$ and the number of spatial elements to be $m = 40$. We have inserted the factor $\frac{1}{120}$ so that, according to Lorenz's estimate, the timescale of the dynamics roughly matches that of a global weather model, with t measured in hours. We use a fourth-order Runge–Kutta scheme for time integration of (10) with time step $\Delta t = 1.5$ hr.

We perform all simulations by assuming a perfect model scenario. That is, a long integration from an arbitrary initial condition is assumed to be the 'true' state. We create the observations, \mathbf{y}^o , by adding uncorrelated random noise with standard Gaussian distribution (mean 0, variance 1) to the true state. To simulate the asynchronous observations, we make 10 uniformly distributed observations at every time step (1.5 hr). We rotate the observation locations so that for every 6 hr period, we make one observation available at each model grid point.

To ensure consistency between the 4D-VAR and 4D-LETKF experiments, the assimilation experiments use the same truth and observations. At each analysis time, we compute the analysis error as the Root Mean Square (RMS) difference between the true state and the analysis ensemble mean for 4D-LETKF (or simply the analysis state for 4D-VAR). Furthermore, we also compute the RMS difference between the mean forecast from the analysis ensemble for 4D-LETKF (or the forecast from 4D-VAR) and the true state at 6 hr intervals up to a 5 d forecast. We then average the analysis errors and the forecast errors over time by taking the RMS over $T/1.5n$ analysis cycles, where the analysis is done every n time steps (1.5n hr) and T is the total length of the simulation. In our simulations, we choose $T = 120\,000$ hr (approximately 13.5 yr). We vary the value of n to examine how the analysis error depends on the time between analyses for 4D-LETKF and on the analysis time window for 4D-VAR.

For the 4D-VAR experiments in this perfect model scenario, we obtain the constant background error covariance matrix \mathbf{B}

for each analysis window iteratively. We initially run 4D-VAR for $T/1.5n$ analysis cycles using an arbitrary background covariance matrix \mathbf{B}_0 and compute the covariance \mathbf{B}_1 of the differences between the true and analysis states at all of the analysis times. Next, we run 4D-VAR using \mathbf{B}_1 as the background error covariance matrix and again compute the covariance \mathbf{B}_2 of the differences between the truth and background. We repeat this process until the average analysis error does not change significantly. To ensure optimality, we then replace the error covariance matrix found by the iterative algorithm, \mathbf{B} , with $\alpha\mathbf{B}$ and tune α to empirically minimize the analysis RMS error. For all analysis windows in this study, α was found to be close to one. This covariance matrix is similar to that used for the constant error covariance for OI by Wang et al. (2006). In this scenario, it provides similar analysis errors to using a covariance matrix generated with the NMC method (Parrish and Derber, 1992).

For 4D-LETKF, we obtain the analysis ensemble at each grid point by computing the 4D-LETKF equations using only the observations within a local region. That is, for each grid point we make a separate computation of (6)–(9) using only the rows and columns of \mathbf{Y}_i and \mathbf{R}_i corresponding to the observations in its region. Following Ott et al. (2004), the local region for a grid point is centred at that grid point and contains a total of 13 grid points. We present results produced from an ensemble of 15 members, as we found that additional ensemble members did not significantly benefit the analysis when using this localization. We apply multiplicative variance inflation, as in (Whitaker and Hamill, 2002), to compensate for the effects of model non-linearity and limited ensemble size. Multiplicative inflation replaces the background covariance matrix \mathbf{P}^b with $(1+r)\mathbf{P}^b$ for some $r > 0$; we do this in LETKF by replacing $(k-1)\mathbf{I}$ with $(k-1)\mathbf{I}/(1+r)$ in (7). We tune r to minimize the analysis RMS error. For these studies, the optimal inflation factor r increased with the length of the analysis window.

We show the average analysis error as a function of the analysis time window in Fig. 1 for 4D-LETKF (solid) and 4D-VAR (dashed). For 4D-LETKF, which should not use the same observation in more than one analysis, the analysis window must correspond to the time between analyses, but for 4D-VAR the time between analyses can be chosen independently of the analysis window. However, for 4D-VAR the analysis window can be chosen independently. We see that the average analysis error of 4D-LETKF grows with the time between analyses, and the average analysis error of 4D-VAR decreases with the length of the analysis window. The 4D-VAR scheme remains stable for a larger range of analysis windows than 4D-LETKF. The mean analysis RMS error of 4D-LETKF appears to saturate at approximately 0.23 for analysis windows between 6 and 24 hr, while for 4D-VAR the mean analysis error appears to approach a similar value for analysis windows between 96 and 108 hr.

For the model we consider here it is computationally feasible to use a large enough ensemble that no localization is necessary. In Fig. 1, we also display results for 4D-LETKF (dot–

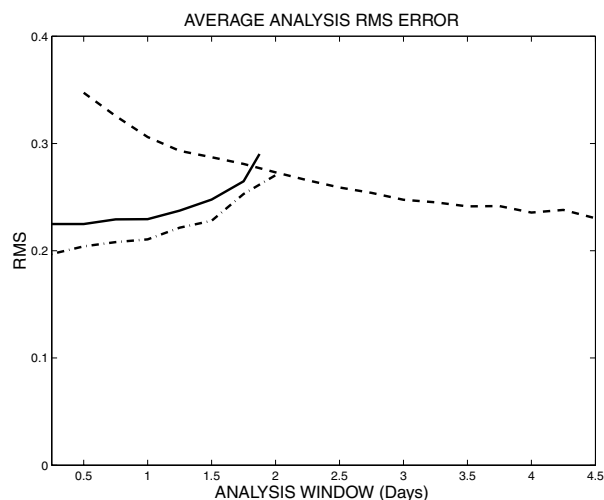


Fig. 1. We show the mean analysis error as a function of analysis window for 4D-VAR (dashed). The mean analysis error is shown as a function for time between analyses for 4D-LETKF with 15 ensemble members and localization (solid) and 50 ensemble members and no localization (dot-dashed). The 15 (50) ensemble member 4D-LETKF experiments used inflation factors of 10% (8%) for the 12 hr, $n = 8$, analysis window, 23% (14%) for the 24 hr, $n = 16$, analysis window, and 65% (24%) for the 42 hr, $n = 28$, analysis window. The 4D-LETKF analysis diverged for all inflation factors below 100% for analysis windows longer than 42 and 48 hr in the 15 and 50 ensemble member experiments, respectively.

dashed) with 50 ensemble members and no localization; that is, the analysis at each grid point uses all of the observations. In this case, the average analysis error is 5–10% better than for the smaller (15 member) ensemble with localization.

To further compare the analysis of 4D-VAR and 4D-LETKF, we compare their average forecast errors as a function of forecast time in Fig. 2. The average forecast error at initial time 0 is the average analysis error. For 4D-VAR we forecast from the 96 hr window analysis (dashed), while for 4D-LETKF we run the forecast from the 24 hr window analysis. For each method, the analysis window we use yields near optimal results (for that method) according to Fig. 1. Because 4D-LETKF provides initial conditions for an ensemble forecast, consider both the mean of an ensemble forecast (solid) and a forecast from the mean analysis state (dot-dashed) to compare with the 4D-VAR forecast. We observe that the 4D-VAR and 4D-LETKF forecasts from the analysis mean have comparable mean RMS errors. The advantage of the ensemble forecast becomes apparent after 2.5 d.

4. Summary

In assimilating the asynchronous observations considered here, 4D-VAR and 4D-LETKF yield comparable average analysis and forecast errors when 4D-VAR is performed with a long enough

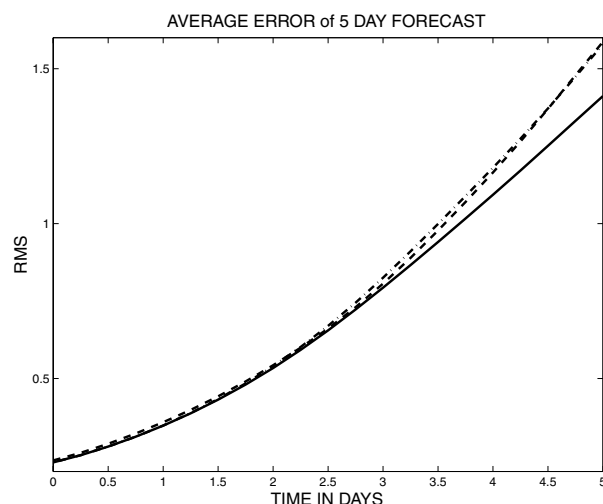


Fig. 2. Mean forecast errors as function of forecast time for 4D-VAR with 96 hr (dashed) and for a 4D-LETKF with 24 hr analysis window using an ensemble forecast (solid) and forecast from the mean analysis state (dot-dashed). The mean analysis error of each scheme is at time 0.

analysis time window and when 4D-LETKF is performed sufficiently frequently. In an operational setting, the time between analyses (and thus the time window for 4D-LETKF) may not be adjustable, while the 4D-VAR analysis window can be chosen as large as computational constraints allow. For the scenario of this paper, our results indicate that if the desired time between analyses is 24 hr or less, the mean analysis from 4D-LETKF with 15 ensemble members is of similar quality to the 4D-VAR analysis with a 96 hr time window. Our results for a 50 member ensemble, shown in Fig. 1, indicate that the loss of accuracy in 4D-LETKF due to a limited ensemble size does not depend significantly on the time between analyses. Since this large ensemble allows for full rank covariances and a global analysis, we presume that the loss of accuracy as the time between analyses increases is due primarily to model non-linearity. While 4D-VAR is not strongly affected by non-linearity, in practice model error will affect both methods. Its effect will increase the errors as the analysis time window grows.

The introduction of model error could further distinguish the two 4D data assimilation schemes. 4D-VAR generally accounts for model error by using the ‘weak constraint formulation’, which adds additional terms of the cost function. In an Ensemble Kalman Filter, additional amounts or different types of variance inflation are generally used to counteract model error. While this is the simplest approach to take in 4D-LETKF, it is also possible to minimize a modified cost function in the space spanned by the ensemble trajectories.

As implemented in this paper, both 4D-VAR and 4D-LETKF assimilate the asynchronous observations at comparable computational cost. However, the implementation of 4D-LETKF can be dramatically sped up by computing the analysis for each

grid point in parallel (Szunoygh et al., 2005). Furthermore, like other Ensemble Kalman Filters, the 4D-LETKF data assimilation scheme is model independent and thus can easily be adapted to new and evolving models without the human cost involved in determining the adjoint of the model for 4D-VAR.

5. Acknowledgments

We thank Joaquim Ballabrera and Aleksey Zimin for their guidance in developing the 4D-VAR code and Eugenia Kalnay and the two anonymous reviewers for their helpful comments. This work was supported by the James S. McDonnell Foundation, the National Science Foundation (grants DMS0104087 and ATM0434225), and NOAA/THORPEX (grant NA04OAR4310104). The first author would also like to acknowledge the support of University of Maryland's Earth System Science Interdisciplinary Center and NASA Goddard Space Flight Center.

References

- Anderson, J. L. 2001. An ensemble adjustment Kalman filter for data assimilation. *Mon. Wea. Rev.* **129**, 2884–2903.
- Bishop, C. H., Etherton, B. and Majumdar, S. J. 2001. Adaptive sampling with the ensemble transform Kalman filter. Part I: Theoretical aspects. *Mon. Wea. Rev.* **129**, 420–436.
- Burgers, G., van Leeuwen, P. J. and Evensen, G. 1998. Analysis scheme in the ensemble Kalman filter. *Mon. Wea. Rev.* **126**, 1719–1724.
- Courtier, P., Thépaut, J. N. and Hollingsworth, A. 1994. A strategy for operational implementation of 4D-VAR, using an incremental approach. *Quart. J. R. Meteorol. Soc.* **120**, 1367–1387.
- Evensen, G. 1994. Sequential data assimilation with a non-linear quasi-geostrophic model using Monte Carlo Methods to forecast error statistics. *J. Geophys. Res.* **99**, 10143–10162.
- Evensen, G. and van Leeuwen, P. J. 2000. An ensemble Kalman smoother for nonlinear dynamics. *Mon. Wea. Rev.* **128**, 1852–1867.
- Houtekamer, P. L. and Mitchell, H. L. 1998. Data assimilation using an ensemble Kalman filter technique. *Mon. Wea. Rev.* **126**, 796–811.
- Houtekamer, P. L., Mitchell, H. L., Pellerin, G., Buehner, M., Charron, M., et al. 2005. Atmospheric data assimilation with the ensemble Kalman filter: Results with real observations. *Mon. Wea. Rev.* **133**, 604–620.
- Houtekamer, P. L. and Mitchell, H. L. 2006. Ensemble Kalman Filtering. *Quart. J. R. Meteorol. Soc.*, in press.
- Hunt, B. R., Kalnay, E., Kostelich, E. J., Ott, E., Patil, D. J. and co-authors. 2004. Four-dimensional ensemble Kalman filtering. *Tellus* **56A**, 273–277.
- Lawson, L.M., Spitz, Y. H., Hofmann, E. E. and Long, R. B. 1995. A data assimilation technique applied to a predator-prey model. *Bull. Math. Biol.* **57**(4), 593–617.
- Le Dimet, F. X. and Talagrand, O. 1986. Variational algorithm for analysis and assimilation of meteorological observations: Theoretical aspects. *Tellus* **38A**, 97–110.
- Lorenc, A. C. 2003. The potential of the ensemble Kalman filter for NWP—a comparison with 4D-VAR. *Quart. J. R. Meteorol. Soc.* **129**, 3183–3203.
- Lorenz, E. N. 1996. Predictability—a problem partly solved. In *Proceedings on predictability, held at ECMWF on 4–8 September 1995*.
- Ott, E., Hunt, B. R., Szunoygh, I., Zimin, A., Kostelich, E. J., and co-authors. 2004. A local ensemble Kalman filter for atmospheric data assimilation. *Tellus* **56A**, 415–428.
- Parrish, D. F. and Derber, J. C. 1992. The National Meteorological Center's spectral statistical-interpolation analysis system. *Mon. Wea. Rev.* **120**(8), 1747–1763.
- Press, W. H., Flannery, B. P., Teukolsky, S. A. and Vetterling, W. V. 1992. *Numerical Recipes in Fortran*. Cambridge University Press, New York.
- Rabier, F., Thépaut, J. N. and Courtier, P. 1998. Extended assimilation and forecast experiments with a four-dimensional variational assimilation system. *Quart. J. R. Meteorol. Soc.* **124**, 1861–1887.
- Rabier, F., Järvién, H., Mahfouf, J. F. and Simmons, A. 2000. The ECMWF operational implementation of four-dimensional variational assimilation: Experimental results with simplified physics. *Quart. J. R. Meteorol. Soc.* **126**, 1148–1170.
- Szunoygh, I., Kostelich, E. J., Gyarmati, G., Patil, D. J., Kalnay, E., and co-authors. 2005. Assessing a local ensemble Kalman filter: Perfect model experiments with the National Centers for Environmental Prediction global model. *Tellus* **57A**, 528–545.
- Wang, X., Bishop, C. H. and Julier, S. J. 2004. Which is better, an ensemble of positive-negative pairs or a centered spherical simplex ensemble? *Mon. Wea. Rev.* **132**(7), 1590–1605.
- Wang, X., Hamill, T.M., Whitaker, J. S. and Bishop, C. H. 2006. A comparison of hybrid ensemble transform Kalman filter–OI and ensemble square-root filter analysis schemes. *Mon. Wea. Rev.*, in press.
- Whitaker, J. S. and Hamill, T. M. 2002. Ensemble data assimilation without perturbed observations. *Mon. Wea. Rev.* **130**, 1913–1924.
- Whitaker, J. S., Compo, G. P., Wei, X. and Hamill, T. M. 2004. Reanalysis without radiosondes using ensemble data assimilation. *Mon. Wea. Rev.* **132**, 1190–1200.
- Whitaker, J. S., Hamill, T. M., Wei, X., Song, Y. and Toth, Z. 2006. Ensemble data assimilation with the NCEP global forecast system. *Mon. Wea. Rev.*, submitted.
- Zupanski, M. 2005. Maximum likelihood ensemble filter: Theoretical aspects. *Mon. Wea. Rev.* **133**, 1710–1726.